



## **Characterization and Improvements to Porous Silicon Processing for Nanoenergetics**

**by Collin Becker, Luke Currano, and Wayne Churaman**

**ARL-TR-4717**

**February 2009**

## **NOTICES**

### **Disclaimers**

The findings in this report are not to be construed as an official Department of the Army position unless so designated by other authorized documents.

Citation of manufacturer's or trade names does not constitute an official endorsement or approval of the use thereof.

Destroy this report when it is no longer needed. Do not return it to the originator.

# **Army Research Laboratory**

Adelphi, MD 20783-1197

---

---

**ARL-TR-4717**

**February 2009**

---

## **Characterization and Improvements to Porous Silicon Processing for Nanoenergetics**

**Collin Becker, Luke Currano, and Wayne Churaman  
Sensors and Electron Devices Directorate, ARL**

# REPORT DOCUMENTATION PAGE

*Form Approved*  
OMB No. 0704-0188

Public reporting burden for this collection of information is estimated to average 1 hour per response, including the time for reviewing instructions, searching existing data sources, gathering and maintaining the data needed, and completing and reviewing the collection information. Send comments regarding this burden estimate or any other aspect of this collection of information, including suggestions for reducing the burden, to Department of Defense, Washington Headquarters Services, Directorate for Information Operations and Reports (0704-0188), 1215 Jefferson Davis Highway, Suite 1204, Arlington, VA 22202-4302. Respondents should be aware that notwithstanding any other provision of law, no person shall be subject to any penalty for failing to comply with a collection of information if it does not display a currently valid OMB control number.

**PLEASE DO NOT RETURN YOUR FORM TO THE ABOVE ADDRESS.**

<b>1. REPORT DATE (DD-MM-YYYY)</b> February 2009		<b>2. REPORT TYPE</b> Final		<b>3. DATES COVERED (From - To)</b> June to August 2008	
<b>4. TITLE AND SUBTITLE</b> Characterization and Improvements to Porous Silicon Processing for Nanoenergetics				<b>5a. CONTRACT NUMBER</b>	
				<b>5b. GRANT NUMBER</b>	
				<b>5c. PROGRAM ELEMENT NUMBER</b>	
<b>6. AUTHOR(S)</b> Collin Becker, Luke Currano, and Wayne Churaman				<b>5d. PROJECT NUMBER</b>	
				<b>5e. TASK NUMBER</b>	
				<b>5f. WORK UNIT NUMBER</b>	
<b>7. PERFORMING ORGANIZATION NAME(S) AND ADDRESS(ES)</b> U.S. Army Research Laboratory ATTN: AMSRD-ARL-SE-RL 2800 Powder Mill Road Adelphi, MD 20783-1197				<b>8. PERFORMING ORGANIZATION REPORT NUMBER</b>  ARL-TR-4717	
<b>9. SPONSORING/MONITORING AGENCY NAME(S) AND ADDRESS(ES)</b>				<b>10. SPONSOR/MONITOR'S ACRONYM(S)</b>	
				<b>11. SPONSOR/MONITOR'S REPORT NUMBER(S)</b>	
<b>12. DISTRIBUTION/AVAILABILITY STATEMENT</b> Approved for public release; distribution unlimited.					
<b>13. SUPPLEMENTARY NOTES</b>					
<b>14. ABSTRACT</b> Nano-porous silicon offers a large surface area to volume ratio typical of nano materials and contains a network of pores that can be filled with oxidant. When a silicon fuel source is combined with an oxidant on the nano-scale, kinetic limitations of silicon oxidation are overcome and an explosive reaction is realized. We present a characterization of lightly doped p-type silicon for nanoenergetic porous silicon (PS) applications. Using gas adsorption measurements and gravimetric techniques, we characterize pore size, porosity, specific surface area, and thickness of PS thin films. Additionally, we report on the energetic reaction of the PS/oxidant system and mechanical stability of PS formed under several etch conditions including varied etch current, drying techniques, and annealing. Prior research has not focused on sample preparation methods of PS for gas adsorption measurements, but results presented here indicate that the method of PS sample preparation for gas adsorption isotherm analysis impacts the results. We find that a newly reported gravimetric technique for PS parameter characterization is inconsistent with expected PS property trends for lightly doped p-type Si.					
<b>15. SUBJECT TERMS</b> Nanoenergetics, porous silicon, gas adsorption					
<b>16. SECURITY CLASSIFICATION OF:</b>			<b>17. LIMITATION OF ABSTRACT</b>  UU	<b>18. NUMBER OF PAGES</b>  20	<b>19a. NAME OF RESPONSIBLE PERSON</b> Luke Currano
<b>a. REPORT</b>  U	<b>b. ABSTRACT</b>  U	<b>c. THIS PAGE</b>  U			<b>19b. TELEPHONE NUMBER (Include area code)</b> 301-394-0566

---

## Contents

---

<b>List of Figures</b>	<b>iv</b>
<b>List of Tables</b>	<b>iv</b>
<b>1. Introduction/Background</b>	<b>1</b>
<b>2. Experiment/Calculations</b>	<b>2</b>
2.1 Porous Silicon Formation and Characterization.....	2
2.2 Oxidizers .....	3
2.3 Porous Silicon Ignition.....	3
<b>3. Results and Discussion</b>	<b>3</b>
3.1 PS Property Characterization .....	3
3.2 Oxidizer and Ignition.....	8
<b>4. Summary and Conclusions</b>	<b>10</b>
<b>5. References</b>	<b>12</b>
<b>Distribution List</b>	<b>14</b>

---

## List of Figures

---

Figure 1. Gas adsorption isotherm of porous silicon (18 mA/cm <sup>1</sup> in 25% HF/EtOH electrolyte). .....	4
Figure 2. BJH adsorption cumulative pore volume of porous silicon (18 mA/cm <sup>2</sup> in 25% HF/EtOH electrolyte). .....	4
Figure 3. BJH adsorption pore volume distribution of porous silicon (18 mA/cm <sup>2</sup> in 25% HF/EtOH electrolyte). .....	5
Figure 4. BJH adsorption mean pore diameter of PS (25% HF/EtOH electrolyte). .....	5
Figure 5. BJH adsorption and gravimetric porosity of PS (25% HF/EtOH electrolyte). .....	6
Figure 6. BJH adsorption and gravimetric porosity of PS (33% HF/EtOH electrolyte). .....	7
Figure 7. BJH adsorption and gravimetric pore diameter of PS (25% and 33% HF/EtOH electrolyte). .....	8
Figure 8. SEM cross section of 9 (left) and 36 (right) mA/cm <sup>2</sup> PS samples. ....	9
Figure 9. 36 mA/cm <sup>2</sup> ignition tests. The chip on the left broke in half, the chip on the right did not. ....	10

---

## List of Tables

---

Table 1. Etch conditions, drying methods, and energetic reaction strength. ....	9
---	---

---

## 1. Introduction/Background

---

The development and tailoring of new energetic materials is critical to the success of explosives, propellants, micro-actuation, and power for next generation DoD weapons and microsystems. Specifically, engineering silicon (Si) for nanoenergetics provides a means to readily integrate energetic material with microsystems. Since the oxidation of Si is much more exothermic than most carbon based materials, it can be engineered to be highly explosive. Furthermore, nanostructured materials can store higher amounts of energy than conventional energetic materials and deliver faster energy release due to their increased surface area.

The nanoenergetic field is relatively young, but already several material systems and processes are being explored (1). However, since Si is inexpensive, well characterized, and the cornerstone of the microelectromechanical systems (MEMS) industry, it will play an important role in this field. If Si can be tailored for the nanoenergetics field, a host of applications will soon follow.

This research work investigates the composite energetic material system of porous silicon (PS) and oxidizer. Current research shows that impregnation of PS with a solid oxidizer leads to a highly exothermic reaction when ignited by high temperature, light, electric or mechanical impulse (1–3). A full suite of material and engineering specific characterizations has yet to be realized however, and the process has yet to be optimized. The most favorable PS growth conditions for energetic applications and a means to efficiently identify PS properties are still being studied (3).

The exothermic reaction of Si with oxygen ( $-911$  kJ/mol), which is far greater than typical carbon-based energetic material, relies on an intimate mixture of oxidant with Si fuel. The diffusion rate of oxygen through the native  $\text{SiO}_2$  on bulk Si, prevents a fast ignition of Si (4). However, with a specifically structured Si thin film that controls pore size, porosity, thickness, and specific surface area, the kinetics of this reaction can be improved.

PS properties are influenced by a number of factors including Si dopant levels, electrolyte composition and concentration, lighting levels, crystal orientation, Si type (N or P), and applied current density. The current literature on nanoenergetic PS has yet to mature, and a careful investigation that explores these variables and uses proven techniques to verify PS properties does not exist. In this work we account for the dopant level, electrolyte composition, current density, and Si type. We then analyze our PS with a gas adsorption method and compare to a newly proposed gravimetric technique (5).

---

## 2. Experiment/Calculations

---

### 2.1 Porous Silicon Formation and Characterization

We produced PS thin films by a constant current electrochemical technique. We used double side polished, lightly doped p-type ( $p^+$ ) wafers (resistivity of 1-30 Ohm-cm). Prior to anodization, we sputtered a Ti/Pt layer on one side of the wafer and annealed in nitrogen for 60 s at 700 °C. This process served to create a backside contact for the wafer. All of our electrolytes are based on 49% HF, and the concentration is reduced to 25% (1 part 49% HF to 1 part EtOH) or 33% (2 parts 49% HF to 1 part EtOH). The ethanol serves to help wet the hydrophobic surface of the Si and aid in removal of  $H_2$  bubbles.

The etching process is performed in a custom-built Teflon cell. The cell is composed of a base and a machined top that is bolted to the base. An o-ring between the base and the top prevents electrolyte leakage. The top half of the cell has a 1.1 cm diameter and 1.6 cm depth cylinder machined out of the Teflon. We place a piece of aluminum foil between the die and the base of the Teflon cell to serve as a backside electrical contact to the Si. We had three identical cells machined and use either a PXI-1042 power supply (National Instruments) or Keithley 2400 source meter power supply to anodically bias the Si die. Unless otherwise noted, all etch times are 30 minutes.

First we scribe our wafers into approximately 2cm x 2cm dice. This serves to contain the electrolyte. Once the top half of the cell is bolted to the base, the cylinder is filled with electrolyte, and a coiled gold (Au) wire that serves as the cathode is immersed just below the level of the electrolyte. The Au wire is parallel to the Si surface and coiled in a manner to increase the surface area of Au in the electrolyte and reduce variations in current density across the Si surface.

After the etch is finished, the cell is rinsed with methanol and the PS is kept immersed in methanol as the cell is taken apart. The PS is then rinsed again in methanol and a thin layer of methanol is allowed to slowly evaporate from the PS. For higher current densities, and low HF concentrations, the PS was rinsed with anhydrous pentane (Sigma Aldrich). Pentane has a much lower surface tension than either methanol or ethanol, and has been shown to reduce PS cracking during drying (Bouchar). Some PS samples are annealed at 300 °C for 1 hour in ambient air.

The gas adsorption measurements are performed according to the BET theory (6–9) and the porosity measurements are calculated with BJH theory (10). A Micromeritics ASAP 2010 with  $N_2$  gas as the adsorbate is used for the analysis. The sample tube for the ASAP 2010 is narrow (less than 10 mm diameter) so our PS die are cleaved prior to inserting into the sample tube. It is necessary to have at least  $10\text{ m}^2$  to analyze, and this corresponds to on the order of 10 die per

measurement. In all experiments we determined the mass of the total sample (bulk Si plus PS). From this, the ASAP 2010 software computed a total volume of gas adsorbed per mass.

Using a Mettler Toledo XP205 micro balance with a repeatability of 0.015 mg and measuring each sample in triplicate, we could record the mass of just the PS. This mass could then be used to compute a total volume of gas adsorbed in just the PS material. We confirmed, by analyzing bulk Si, that the volume of gas adsorbed by the bulk Si is insignificant (0.6%). The end result is that no errors result from analyzing a composite PS/bulk Si material, and the gas adsorption values correspond only to PS.

To confirm the gravimetric method (5) removal of the PS is necessary. We use a 5% KOH etch solution (5) to remove the PS thin and we record the etch depth with a Veeco optical profilometer. SEM images are used to independently verify the etch depth.

## **2.2 Oxidizers**

For all oxidizer tests,  $\text{NaClO}_4$  (Sigma Aldrich) is used and is dissolved in either methanol or anhydrous ethanol. The oxidizers are applied (the pores are filled) by dropping oxidizer solution with a pipette directly on the PS. In all, cases we fill the pores with two drops of solution. This is enough solution to completely cover the PS region. If a multi-step filling procedure is used, the first two drops are allowed to visually dry before applying additional drops. The solution dries in a humidity controlled box flooded with  $\text{N}_2$  gas to reduce the humidity to about 30%.

## **2.3 Porous Silicon Ignition**

PS is ignited either by an electric spark, supplied by shorting two wires above the PS surface, or by a passing a current through a bridge wire made by a shadow mask deposition method. The ignition is recorded on a Canon PowerShot SD500 camera (future studies will include the use of a high-speed camera).

---

# **3. Results and Discussion**

---

## **3.1 PS Property Characterization**

Our primary focus is to characterize the processing properties of PS that will allow for the most effective oxidant incorporation and subsequent energetic reaction. The analysis of gas adsorption isotherms has been widely used to determine porosity and pore size distributions in PS (11). Figure 1 shows a result from a sample of PS prepared with a current density of  $18 \text{ mA/cm}^2$  for 30 minutes in 25% HF/EtOH electrolyte.

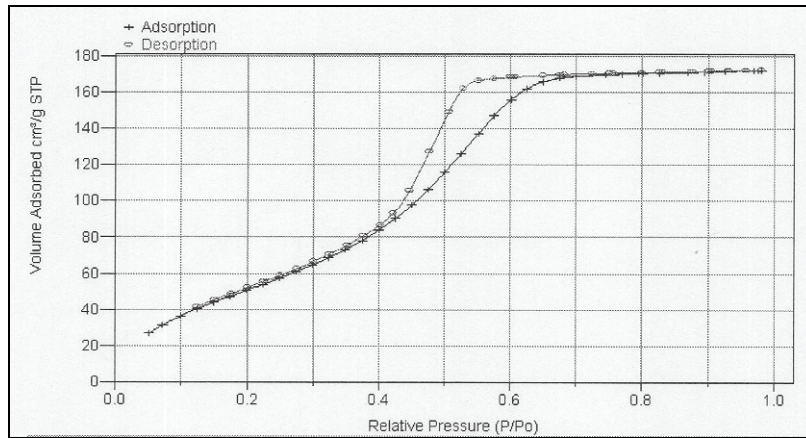


Figure 1. Gas adsorption isotherm of porous silicon ( $18 \text{ mA/cm}^1$  in 25% HF/EtOH electrolyte).

The gas adsorption method begins with  $\text{N}_2$  adsorption inside the pores up to a partial pressure of about 0.4. At higher partial pressures, the  $\text{N}_2$  actually begins to condense in the pores, and the curve continues until a plateau is reached that indicates all of the pores have been filled. Upon desorption, a hysteresis results from the inherently different conditions of desorption compared to adsorption (11). For the case of lightly doped p-type Si, the microstructure of the material is observed to be an interconnected fine pore structure (9). In such a system, it is recommended that the adsorption curve be used for pore size analysis (9). The thermodynamical approach known as the BJH method is used to analyze the isotherms and obtain a pore size distribution (8, 10).

Figures 2 and 3 present the pore size distribution versus the cumulative pore volume and the change in volume divided by the change in pore size ( $dV/dD$ ) respectively.

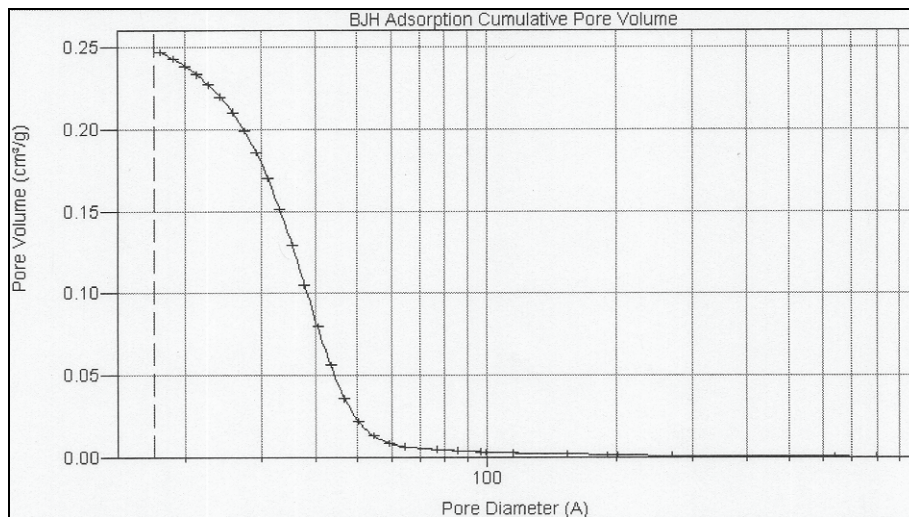


Figure 2. BJH adsorption cumulative pore volume of porous silicon ( $18 \text{ mA/cm}^2$  in 25% HF/EtOH electrolyte).

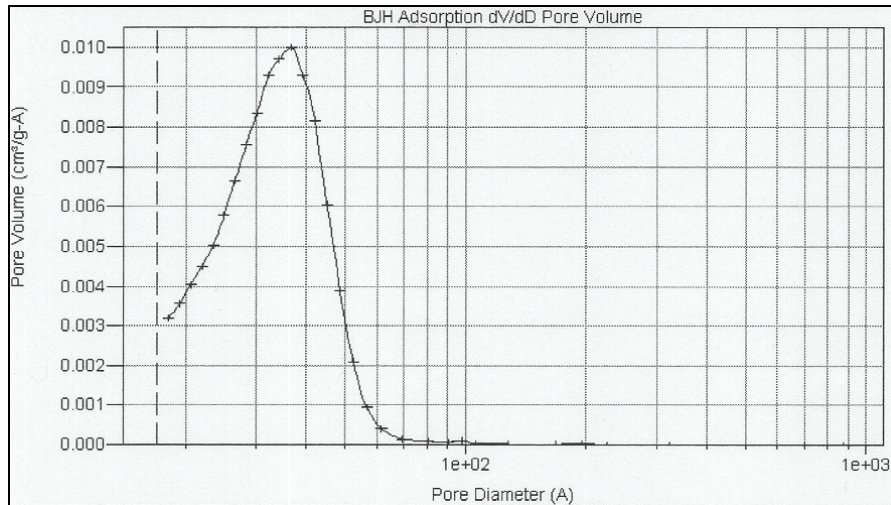


Figure 3. BJH adsorption pore volume distribution of porous silicon (18 mA/cm<sup>2</sup> in 25% HF/EtOH electrolyte).

Figure 4 presents the pore diameters formed in 25% and 33% HF/EtOH electrolyte. The trend of increasing pore size with current density follows expected results (6).

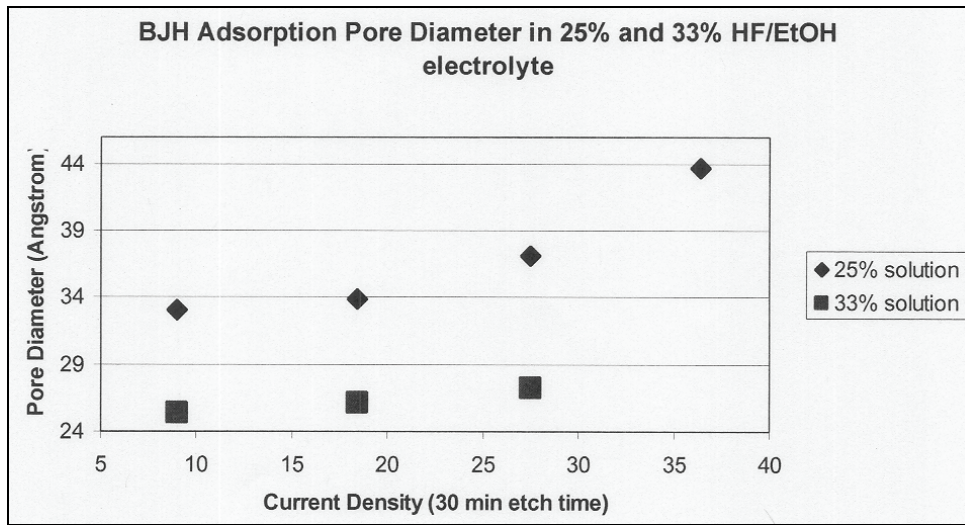


Figure 4. BJH adsorption mean pore diameter of PS (25% HF/EtOH electrolyte).

Ruike et al. in (9) demonstrates on a 20 Ohm-cm Si sample, a mean pore diameter of 3.1 nm, and a much broader distribution of pore sizes (1.8–5.2 nm) at 10 mA/cm<sup>2</sup> compared to our results. However, Ruike prepared 150 μm thick PS layers compared to our 17 μm thick thin films. Especially in low concentration HF solutions (25% HF or less), a dramatic broadening of pore size range occurs (11). Ruike does not note a specific etch time, but certainly it was on the order of hours and not minutes and it quite possible the PS network was attacked as hydroxide ions in solution competed to form an oxide layer in the PS network that would be subsequently etched

by HE. Canham (11) specifically reports an increase in pore size for the same current density, electrolyte concentration, wafer resistivity, but increased etch time.

Additionally, Ruike notes that at the end of the etch, the PS layer was removed from the Si substrate by a high current blast that served to electropolish the Si underneath and remove the PS layer. We have tried a similar approach using a 18 mA/cm<sup>2</sup> samples. Our work shows that the mean pore diameter increases from 3.3 to 4.5 nm in this method. Authors seem to differ in their approach on preparing samples for gas adsorption measurement, specifically if they render free-standing PS films, or measure the PS film with the bulk Si substrate (6, 8, 9). To our knowledge there no articles reporting on pore size distributions of free standing PS compared to PS incorporated in bulk Si.

Increasing the concentration of HF will result in a mean pore diameter decrease (11). As figure 4 shows, for 33% HF, the mean pore diameter is reduced compared to the 25% HF electrolyte. Pore diameter does increase with current density as expected.

From gas adsorption isotherms the porosity of the layers can be deduced (8, 9). Our gas adsorption results for porosity correspond closely to those attained from the proven gravimetric method for porosity determination (8). Figures 5 and 6 show the porosity results.

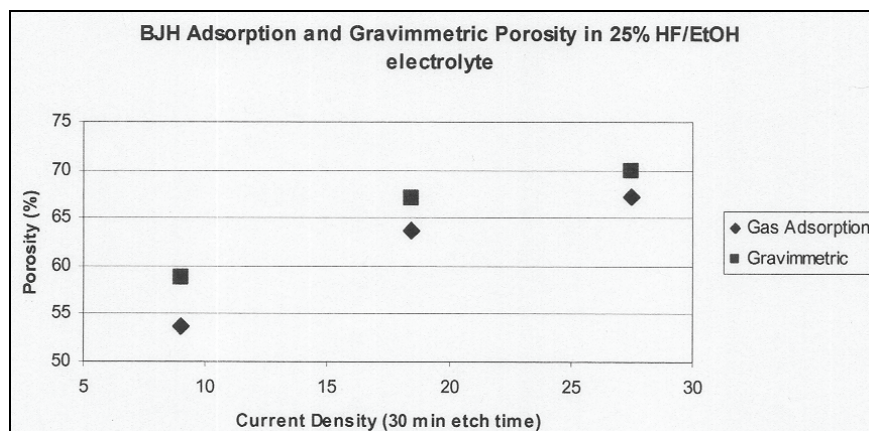


Figure 5. BJH adsorption and gravimetric porosity of PS (25% HF/EtOH electrolyte).

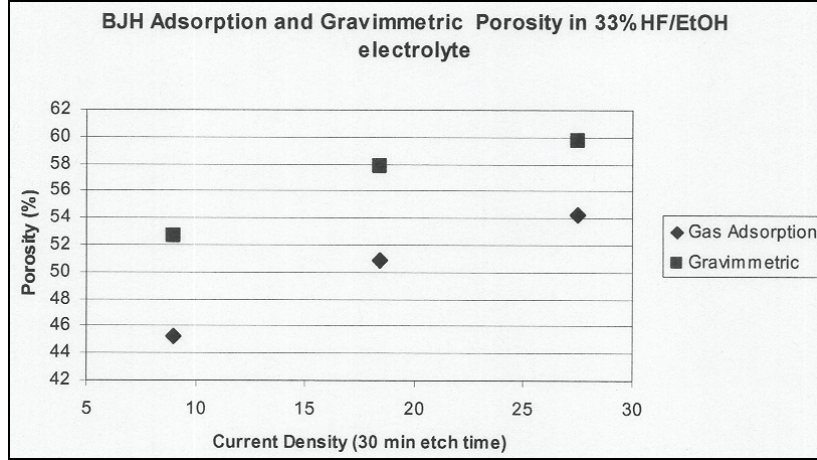


Figure 6. BJJ adsorption and gravimetric porosity of PS (33% HF/EtOH electrolyte).

The porosity was independently determined by gravimetric analysis as well. In the gravimetric analysis, the mass of the die prior to anodization ( $m_1$ ), the mass of the die after anodization ( $m_2$ ), and the mass of the die after removal of the PS layer in 5% KOH ( $m_3$ ) are recorded. The porosity is given by equation 1.

$$\frac{m_1 - m_2}{m_1 - m_3} 100\% \quad (1)$$

The gravimetric method of porosity determination is the standard, even when gas adsorption isotherm analysis is available. The gas adsorption results seem to underestimate porosity slightly compared to the standard of gravimetric measurement. One possible explanation is that some PS mass is lost during transfer to the gas adsorption sample tube, while this will not affect pore size distribution results, porosity values will be affected.

Recently, reports of a gravimetric method to determine mean pore size have been presented (5, 12). Briefly, this technique involves recording  $m_{1,2,3}$  as well as the change in mass after immersion in a 5% HF/EtOH solution. The change in mass is recorded after each 3 minute etch and a total of 4 etches are performed. From a known Si etch rate in 5% HF, a new porosity is recorded (13). Finally, a unit cell PS structural model is proposed and the changing porosity with etch time is used to calculate a unit cell size and corresponding pore size.

We have attempted this analysis, and while the results are on the order of magnitude of the gas adsorption results, we do not find agreement with the two methods for lightly doped p-type wafers. One major discrepancy is that gravimetric calculations show an increasing pore size with increasing electrolyte concentration, a result that is inconsistent with both literature reports and our gas adsorption analysis. Figure 7 shows the pore sizes from the two methods in the two electrolytes.

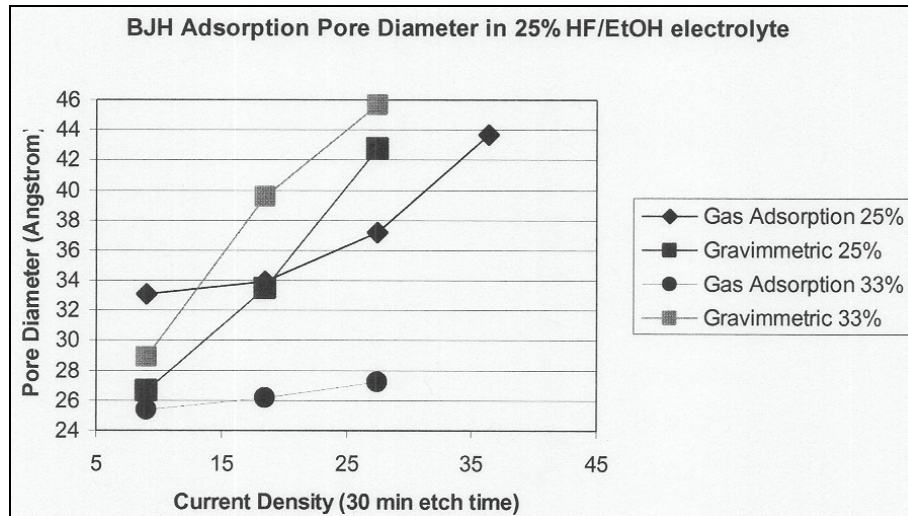


Figure 7. BJH adsorption and gravimetric pore diameter of PS (25% and 33% HF/EtOH electrolyte).

It is not surprising that the gravimetric results disagree with the gas adsorption results. Currently, this new gravimetric technique is unproven, and the authors that report the technique give limited supporting evidence for its accuracy. The method is confounded by the use of different doped wafers, different etch times, and different etch currents.

Since we are using lightly doped P-type wafers, the characterization of PS properties is difficult. The PS microstructure of such wafers is known to be a fine pore structure and highly branched. The literature indicates that the gas adsorption analysis is valid for such a structure, while the gravimetric technique is unproven. The advantages of a gravimetric technique to confirm pore parameters involve a slightly reduced measurement time and reduction in the amount of PS required for the measurement. While a gas adsorption instrument is not required, a highly accurate and expensive balance is needed, and recording the mass after each etch is tedious and time consuming.

### 3.2 Oxidizer and Ignition

From past work at ARL, it has been determined that PS samples prepared at 18 mA/cm<sup>2</sup> and filled with a saturated solution of NaClO<sub>4</sub> in ethanol result in the most dramatic exothermic reactions. As of yet, no groups have reported an experimentally measured value for the energy released upon ignition of PS/oxidant. Researchers, however, report qualitative results from sight and sound. In principle, a sample with the largest specific surface area is desired to produce the most exothermic reaction. However, the porosity and pore size are important in that highly porous samples are mechanically unstable and if the pore size is too small the oxidizer cannot fill the pores. It is thought that a pore diameter on the order of 3.5 nm is optimal for PS energetic (5).

Recently we have found that samples etched at 36 mA/cm<sup>2</sup> show a pronounced increase in reaction energy over our previous work with 18 mA/cm<sup>2</sup> samples. This current density corresponds to a thickness of 57.5 μm and pore diameter of 4.4 nm. At this etch current however, the layers are mechanically unstable. Two methods to reduce the instability have been investigated: tapering the etch current density and pentane drying.

Figure 8 shows SEM cross sections of 9 and 36 mA/cm<sup>2</sup> PS layers respectively.

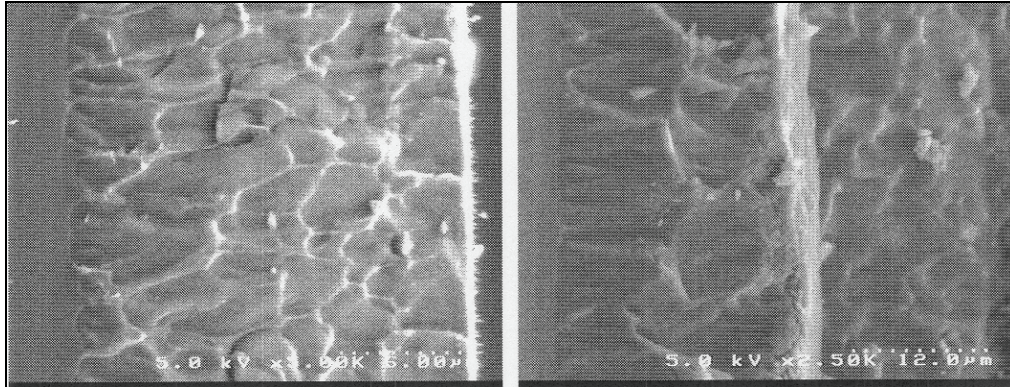


Figure 8. SEM cross section of 9 (left) and 36 (right) mA/cm<sup>2</sup> PS samples.

It is thought that by tapering the etch, a finer pore structure can be realized at the Si/PS boundary, and the PS can be anchored better to the substrate. Additionally, the residual stress created from transitioning to a large pore diameter to the bulk Si, may be reduced by decreasing the pore diameter with time.

We have found that a die etched at 36 mA/cm<sup>2</sup> for 30 minutes in 25% HF is unstable after drying, although this can be reduced with pentane drying. However, a die that is anodized for 30 min at 36 mA/cm<sup>2</sup>, then reduced to 27 mA/cm<sup>2</sup> for 5 minutes, then to 18 mA/cm<sup>2</sup> for 5 minutes is mechanically stable after drying, even without the aid of pentane. Additionally we find that reducing to 18 mA/cm<sup>2</sup> for 5 minutes then to 9 mA/cm<sup>2</sup> is stable, but simply reducing to 9 mA/cm<sup>2</sup> is not stable even with pentane drying. It is worthy to note that in 33% HF/EtOH solutions, layers are stable up to 100 mA/cm<sup>2</sup>. Table 1 summarizes our results.

Table 1. Etch conditions, drying methods, and energetic reaction strength.

Electrolyte Composition	25% HF/EtOH						
	9	18	27	36	36	36	36
Initial current density mA/cm <sup>2</sup>	9	18	27	36	36	36	36
Initial etch time	30	30	30	30	30	30	30
Current reduction 1 (5 min)	na	na	na	na	na	27	18
Current reduction 2 (5 min)	na	na	na	na	na	18	9
Pentane drying	n	n	n	n	y	n	n
Anneal (y/n)	n	n	n	n	y	n	n
Stable layer (y/n)	y	y	y	n	y	y	y
Layer stable after oxidant filling	y	y	y	n	y	n	n
Reaction	na	moderate	na	strong	weak	strong	strong

Table 1 also indicates whether a PS layer cracked after filling with the oxidant solution. While the layers may be stable after initial drying, maintaining their integrity after the oxidant solution is deposited is difficult. Despite PS layer cracking, strong exothermic reactions are realized. Annealing at 300 °C for one hour did stabilize the layer, but the resulting reaction was very weak. The PS layer grows an oxide layer in these annealing conditions that may be inhibiting the reaction strength. A benefit, however, is that the PS becomes hydrophilic under these conditions and while it may also be inhibiting pore filling, it may allow for water soluble oxidants to be introduced to the pores. Annealing at lower temperatures has yet to be tested, but it is reported that at 250 °C the reactivity is not affected (2).

Videos of the ignition tend to show either a large flame or blue plasma-like halo. Since we are not recording with a high speed camera, the blue plasma-like halo could be a matter of not having the speed to catch a fast moving flame. Our most energetic reaction to date of a 36 mA/cm<sup>2</sup> die is shown in figure 9 on the left. In this reaction the die broke in half. Figure 9 on the right shows another strong reaction with a flame visible, but the die did not break.



Figure 9. 36 mA/cm<sup>2</sup> ignition tests. The chip on the left broke in half, the chip on the right did not.

---

## 4. Summary and Conclusions

---

We have carried out a deliberate investigation into the properties of PS formed on lightly doped p-type wafers. Primarily we are interested in characterizing PS to develop the most efficient energetic reaction. A gas adsorption method and a gravimetric method were both used to investigate PS properties. The gravimetric method produces results that do not correlate with expected trends from the literature. However, the results are on the same order of magnitude as those from the gas adsorption method. We have found that increasing the pore size from our initial test set of PS layers has produced more energetic reactions, but at the cost of layer stability.

In the short-term, new work will focus on comparing gas adsorption results to gravimetric results from standard doped p-type wafers. Furthermore, different electrolyte compositions will be investigated, as well as the incorporation of surfactants to both maximize layer stability during drying and during incorporation of oxidant.

---

## 5. References

---

1. Rossi, C.; Zhang, K.; Esteve, D.; Alphonse, P.; Tailhades, P.; Vahlas, C. Nanoenergetic materials for MEMS: A review. *Journal of Microelectromechanical Systems* **2007**, *16*, 919–931.
2. Clement, D.; Diener, J.; Gross, E.; Kunzner, N.; Timoshenko, V. Y.; Kovalev, D. Highly explosive nanosilicon-based composite materials. *Physica Status Solidi a-Applications and Materials Science* **2005**, *202*, 1357–1364.
3. du Plessis, M. Nanoporous silicon explosive devices. *Materials Science and Engineering B-Solid State Materials for Advanced Technology* **2008**, *147*, 226-229.
4. Kovalev, D.; Timoshenko, V. Y.; Kunzner, N.; Gross, E.; Koch, F. Strong explosive interaction of hydrogenated porous silicon with oxygen at cryogenic temperatures. *Physical Review Letters* **2001**, *87*.
5. du Plessis, M. Relationship between specific surface area and pore dimension of high porosity nanoporous silicon - Model and experiment. *Physica Status Solidi a-Applications and Materials Science* **2007**, *204*, 2319–2328.
6. Bomchil, G.; Herino, R.; Barla, K.; Pfister, J. C. Pore-Size Distribution in Porous Silicon Studied by Adsorption-Isotherms. *Journal of the Electrochemical Society* **1983**, *130*, 1611–1614.
7. Buriak, J. M.; Stewart, M. P.; Geders, T. W.; Allen, M. J.; Choi, H. C.; Smith, J.; Raftery, D.; Canham, L. T. Lewis acid mediated hydrosilylation on porous silicon surfaces. *Journal of the American Chemical Society* **1999**, *121*, 11491–11502.
8. Herino, R.; Bomchil, G.; Barla, K.; Bertrand, C.; Ginoux, J. L. Porosity and Pore-Size Distributions of Porous Silicon Layers. *Journal of the Electrochemical Society* **1987**, *134*, 1994–2000.
9. Ruike, M.; Houzouji, M.; Motohashi, A.; Murase, N.; Kinoshita, A.; Kaneko, K. Pore structure of porous silicon formed on a lightly doped crystal silicon. *Langmuir* **1996**, *12*, 4828–4831.
10. Barrett, E. P.; Joyner, L. G.; Halenda, P. P. The Determination of Pore Volume and Area Distributions in Porous Substances .1. Computations from Nitrogen Isotherms. *Journal of the American Chemical Society* **1951**, *73*, 373–380.
11. Canham, L. T. *Properties of Porous Silicon*; Institution of Engineering and Technology, 1997.

12. du Plessis, M. Properties of porous silicon nano-explosive devices. *Sensors and Actuators a-Physical* **2007**, *135*, 666–674.
13. Halimaoui, A. Determination of the Specific Surface-Area of Porous Silicon from its Etch Rate in Hf Solutions. *Surface Science* **1994**, *306*, L550–L554.

NO. OF COPIES	ORGANIZATION	NO. OF COPIES	ORGANIZATION
1 ELEC	ADMNSTR DEFNS TECHL INFO CTR ATTN DTIC OCP 8725 JOHN J KINGMAN RD STE 0944 FT BELVOIR VA 22060-6218	1	US ARMY RSRCH LAB ATTN AMSRD ARL CI OK TP TECHL LIB T LANDFRIED BLDG 4600 ABERDEEN PROVING GROUND MD 21005-5066
1	DARPA ATTN IXO S WELBY 3701 N FAIRFAX DR ARLINGTON VA 22203-1714	1	DIRECTOR US ARMY RSRCH LAB ATTN AMSRD ARL RO EV W D BACH PO BOX 12211 RESEARCH TRIANGLE PARK NC 27709
1 CD	OFC OF THE SECY OF DEFNS ATTN ODDRE (R&AT) THE PENTAGON WASHINGTON DC 20301-3080		
1	US ARMY RSRCH DEV AND ENGRG CMND ARMAMENT RSRCH DEV AND ENGRG CTR ARMAMENT ENGRG AND TECHNLGY CTR ATTN AMSRD AAR AEF T J MATTS BLDG 305 ABERDEEN PROVING GROUND MD 21005-5001	13	US ARMY RSRCH LAB ATTN AMSRD ARL CI OK PE TECHL PUB ATTN AMSRD ARL CI OK TL TECHL LIB ATTN AMSRD ARL SE RL L CURRANO (5 COPIES) ATTN AMSRD ARL SE RL W CHURAMAN (5 COPIES) ATTN IMNE ALC HR MAIL & RECORDS MGMT ADELPHI MD 20783-1197
1	PM TIMS, PROFILER (MMS-P) AN/TMQ-52 ATTN B GRIFFIES BUILDING 563 FT MONMOUTH NJ 07703		
1	US ARMY INFO SYS ENGRG CMND ATTN AMSEL IE TD F JENIA FT HUACHUCA AZ 85613-5300		
1	COMMANDER US ARMY RDECOM ATTN AMSRD AMR W C MCCORKLE 5400 FOWLER RD REDSTONE ARSENAL AL 35898-5000		
1	US GOVERNMENT PRINT OFF DEPOSITORY RECEIVING SECTION ATTN MAIL STOP IDAD J TATE 732 NORTH CAPITOL ST NW WASHINGTON DC 20402		
			TOTAL: 23 (1 ELEC, 1 CD, 21 HCS)